Optics & Laser Technology 156 (2022) 108545

Contents lists available at ScienceDirect

Optics and Laser Technology

journal homepage: www.elsevier.com/locate/optlastec

Full length article

Liquid crystal optical fiber sensor based on misaligned core configuration for temperature and mixed volatile organic compound detection

Dong Zhou [a], Zeqing Lan [a], Wenzhu Cao [a], Yuzhou Chen [a], Shushen Zhang [c,*], Jianyang Hu [a], Jianyu Shang [a], Zenghui Peng [b], Yongjun Liu [a,b,*]

[a] Key Lab of In-fiber Integrated Optics, Ministry Education of China, Harbin Engineering University, Harbin 150001, China
[b] State Key Laboratory of Applied Optics, Changchun Institute of Optics, Fine Mechanics and Physics, Chinese Academy of Sciences, Changchun 130033, China
[c] TYW Electronics Co., Ltd, Suihua, Heilongjiang 150038, China

ARTICLE INFO

Keywords:
Liquid crystal
Optical fiber
Volatile organic compound

ABSTRACT

In this paper, an optical fiber sensor based on cholesteric liquid crystal (CLC) is used for real-time monitoring of temperature and volatile organic compound (VOC) gas concentration. The sensor works based on a 2 × 2 multimode fiber coupler whose two output ports can respectively function as gas and temperature sensor probes. The former was realized by dislocation fusion of two multimode fibers (MMFs) coated with two CLCs, and the CLC reflection peak has a red shift with the increasing concentrations of acetone and tetrahydrofuran (THF) gas. The other MMF port has been fused with hollow capillary fibers (HCF). To eliminate the adverse effects of external temperature fluctuations, the enclosed CLC in the HCF will realize real-time temperature monitoring and temperature compensation. In addition, the sensor can also measure the dependence of the wavelength on the total gas concentration of different mixing ratios of acetone and THF, and distinguish the concentration of acetone and THF in the mixed gas.

1. Introduction

Volatile organic compounds (VOCs) are common gaseous pollutants in the air. Acetone and tetrahydrofuran (THF) are relatively important organic solvents and raw materials for organic synthesis. At the same time, they are the main chemical components in the pharmaceutical waste liquid that are difficult to separate and recover under normal pressure [1]. In the pharmaceutical industry, the mixture of acetone and tetrahydrofuran is used to dissolve drug molecules, and its separation and purification [2] also involve problems such as solvent volatilization. Therefore, sensors for real-time monitoring of VOC gas concentration in chemical and pharmaceutical applications are desirable. By now, technologies for detecting VOC gases have been proposed, such as gas chromatography-mass spectrometry (GC-MS) [3], resistive-based gas sensors [4] and ion mobility spectrometry [5]. Although these methods have high sensitivity and accuracy for VOC gas detection, but they have disadvantages such as expensive and huge facilities, complicated experimental preparations, and difficulty in real-time VOC detection. Therefore, optical fiber sensors have the advantages of low cost, fast response and ultra-compactness in VOC gas detection [6].

Liquid crystals (LCs) are soft materials that can respond quickly to external stimuli. The properties of LC change under the effect of the surrounding environment and substances, including biological cell detection [7–9], electric field [10–12], pH [13,14], polarization imaging [15] and volatile gases [16,17]. At the same time, LC is also sensitive to temperature, so it is often used for temperature sensor [18,19]. Cholesteric liquid crystal (CLC) has the characteristics of self-assembled spiral structure and selective reflection. Under the action of chiral molecules [20], rod-shaped LC molecules self-assemble to form a helical structure, and the distance along the helical axis reaches a pitch as the LC directors rotate 2π. The change of pitch causes wavelength shifts of the CLC selective reflection. For several CLC-based VOC gas sensors [21,22], they can only qualitatively analyze the gas concentration based on reflecting color changes of CLC films. These gas sensors are poor at being used in real environments, and they are also affected by temperature when detecting VOC gas. As the carrier of liquid crystal, the optical fiber is not only small in size but also can monitor the gas concentration from a long distance, which can effectively reduce the harm to the human body.

In this work, we reported sensors works on a 2 × 2 multimode fiber coupler whose two output ports can respectively function as gas and

* Corresponding authors at: Key Lab of In-fiber Integrated Optics, Ministry Education of China, Harbin Engineering University, Harbin 150001, China (Y. Liu).
E-mail addresses: shushen.zhang@hljtyw.com (S. Zhang), liuyj@hrbeu.edu.cn (Y. Liu).

https://doi.org/10.1016/j.optlastec.2022.108545
Received 4 April 2022; Received in revised form 15 June 2022; Accepted 28 July 2022
Available online 12 August 2022

Table 1
The ratio of three CLCs.

	Agentia 1	Agentia 2	Agentia 3	RM257	Irgacure369
CLC1	10 wt%	70 wt%	20 wt%	/	/
CLC2	13.7 wt%	61.6 wt%	20.7 wt%	3 wt%	1 wt%
CLC3	20.6 wt%	54.8 wt%	20.6 wt%	3 wt%	1 wt%

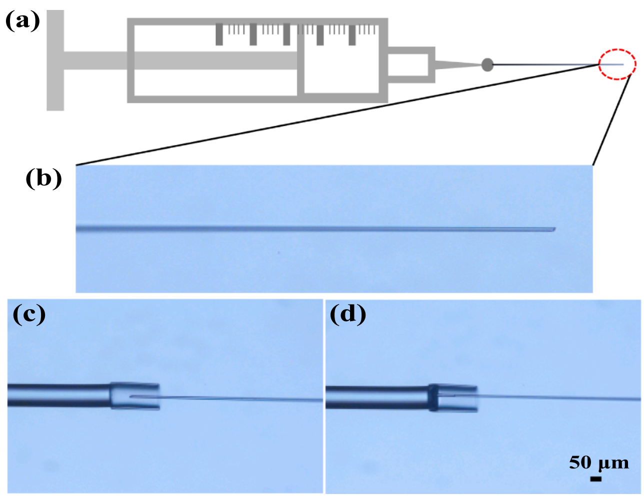

Fig. 1. (a) Schematic of the microtube structure. (b) Micrograph of the microtube tip. (c) and (d) Micrograph of CLC injection process. The scale bar is 50 μm.

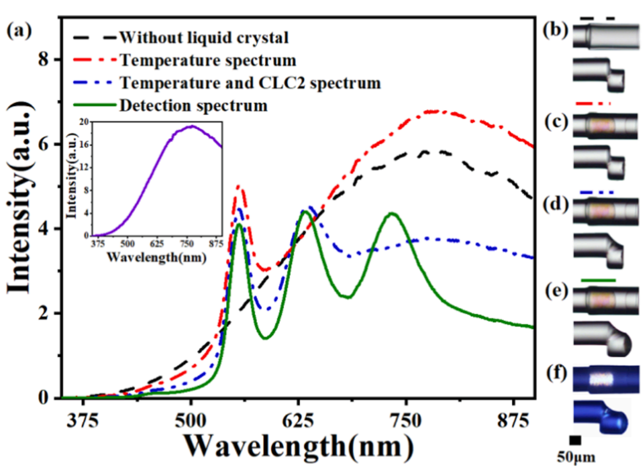

Fig. 2. (a) Different reflection spectra during the fabrication of the sensor. The illustration shows the spectrum of the original light source. Corresponding two probes under the bright field microscope (b) without CLCs, (c) with CLC1, (d) with CLC1 and CLC2, (e) with CLC1, CLC2 and CLC3. (f) Complete sensor under the polarizing optical microscope. The scale bar is 56 μm.

temperature sensor probes. The former was realized by dislocation fusion of two multimode fibers (MMFs) coated with two CLCs. The other MMF port has been fused with hollow capillary fibers (HCF). To eliminate the adverse effects of external temperature fluctuations, the enclosed CLC in the HCF will realize real-time temperature monitoring and temperature compensation. As the concentrations of acetone and THF gas increase, the reflected wavelength of CLC will be red-shifted, and the temperature compensation effect of the sensor was.

explored. When the temperature is unchanged, a single optical fiber can be used to measure the mixed gas, which is more practical. At the same time, the sensor can also distinguish the ratio of acetone and THF.

2. Materials and methods

Cholesterol chloroformate, cholesteryl oleyl carbonate and cholesterol chloride, cross-linkable liquid crystal monomer Benzoic acid, 4-[3-[(1-oxo-2-propen-1-yl)oxy]propoxy]-,1,1′-(2-methyl-1,4-phenylene) ester (RM257), photoinitiator 2-Benzyl-2-(dimethylamino)-4′-morpholinobutyrophenone (Irgacure369) were purchased from Beijing InnoChem. Polyglycerin-10 was purchased from Shandong Yousuo Chemical Technology Co., Ltd. UV curing glue (LEAFTOP 9310) was purchased from Shenzhen Tegu New Material Co., Ltd.. Considering the range of light sources and avoiding cross-reflection spectra, the three CLC ratios are shown in Table 1. Among them, Agentia 1, Agentia 2 and Agentia 3 represent cholesterol chloroformate, cholesterol oleyl carbonate and cholesterol chloride, respectively. After producing these three CLCs, they were heated at 110 °C for 20 mins, sonicated at 75 °C for 30 mins, and then cooled to room temperature naturally.

The temperature sensing probe was prepared by welding the HCF to MMF with a fusion splicer (FSM-80S, from Fujikura). The outer diameter of HCF (TSP100375, from Innosep) is 140 μm. The inner diameter is 100 μm. The length is about 250 μm. The outer diameter of MMF is 125 μm, and the core diameter is 105 μm. Then the CLC1 (Film thickness is 100 μm), polyglycerin-10 (Shandong Yousuo Chemical Technology Co., Ltd.) and UV curing glue (LEAFTOP 9310) were sequentially injected into HCF through a tapered microtube (about 10 μm in diameter) and were subjected to UV polymerization for 10 mins at an intensity of 20 mW/m^2. The tapered microtube was made by flame heating and taper technology, and the microtube was connected to the syringe to draw or inject liquid at will, as shown in Fig. 1. Tapered microtubes were used to quantitatively absorb CLC, which is convenient for precise control of the thickness of the LC under the microscope. The preparation of the VOC sensing probe was misaligning the cores of two MMFs by welding, and cutting it to a suitable length under the microscope, and its fiber end has not been treated. Some CLC2 and CLC3 (Film thickness is 40 μm) were put on two end faces and subjected to UV polymerization at the same intensity for 2 mins. Fig. 2 illustrates the manufacturing operation and corresponding reflection spectra of two probes. The inset of Fig. 2(a) is the light source spectrum. The black line represents the original spectrum with no CLCs in the fiber structure. As shown in Fig. 2(a) and 2(b), these fiber ends have only about 4 % low reflectivity [23], so the reflected spectrum is much less intense than the light source spectrum. CLC has anisotropy and spiral twisting direction, and its molecules are arranged layer by layer, and the average orientation of each layer of molecules rotates by an angle. This kind of periodic CLC can be regarded as the Bragg structure, and its periodic structure allows reflecting light selectively in a reflection bandwidth of $\Delta\lambda = \Delta n p$ [24], where $\Delta n = n_e$-n_o is the refractive index difference of the LC, and p is the pitch. Fig. 2(c) is the image of the sensor filled with CLC1 for temperature measurement, and the corresponding reflection spectrum is the red line. Fig. 2(d) and Fig. 2(e) are micrographs of coated CLC2 and CLC3, respectively. The corresponding spectra of these two liquid crystals are the blue and green lines, respectively. Finally, the three reflected wavelengths for real-time temperature and gas monitoring are 560 nm, 660 nm and 745 nm respectively.

The configuration of the experimental system is shown in Fig. 3(a). The tungsten-halogen lamp (HL2000, Ideaoptics Inc., input power 9 W) is employed as the light source and launches white light into a port (port 2) of a 2 × 2 MMF coupler. The VOC gas probe (port 4) and the temperature probe (port 3) are fixed into a gas chamber. The reflected light from the sensor probe is collected through a coupler and sent to an optical spectrum analyzer (QEpro, Ocean Optics Inc., spectral range of 300–1100 nm and resolution of 0.14 nm) by port 1. A computer is used to monitor, record, and analyze the reflection spectra. A schematic diagram of the temperature probe is shown in Fig. 3(b). A schematic diagram of a VOC gas sensing probe is shown in Fig. 3(c). CLC2 and CLC3 firmly adhered to the fiber end after UV curing of RM257 mixed in them. A certain amount of VOC was titrated with a micro syringe into the gas

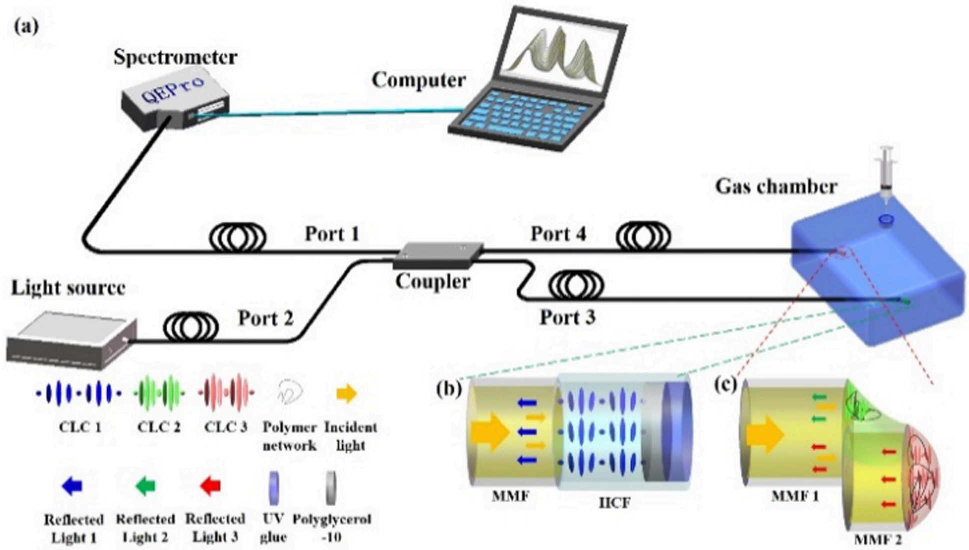

Fig. 3. (a) Schematic of temperature-compensated optical fiber VOC gas sensing device. (b) Schematic diagram of temperature probe and (c) VOC gas probe.

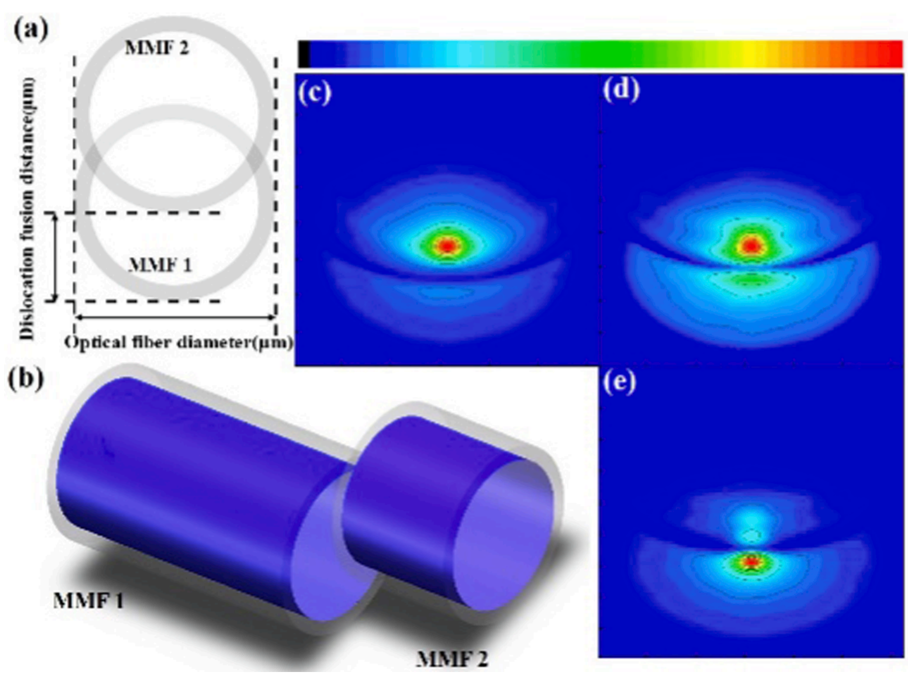

Fig. 4. Simulation diagram of optical fiber VOC gas probe without CLCs. (a) Schematic diagram of the dislocation fusion plane. (b) 3D schematic diagram of dislocation fusion fiber. Energy analysis of dislocation fusions (c) 46 μm, (d) 56 μm and (e) 66 μm. The length of MMF2 is 95 μm.

chamber, and the sensor detected the change in gas concentration. The sensor detected VOC three times and then conducted data analysis and statistics. When the concentration or ratio of acetone and THF changes, the reflected wavelength position changes according to the variation of CLC pitch.

3. Results and discussion

In order to verify the energy distribution incident to the LC films and select the appropriate deviation. This paper carried out a simulating calculation by the ray-tracing method. The light source is a halogen light source with a power of 9 W and a light source diameter of 8 mm. The light source was then coupled to the fiber through a lens with a diameter

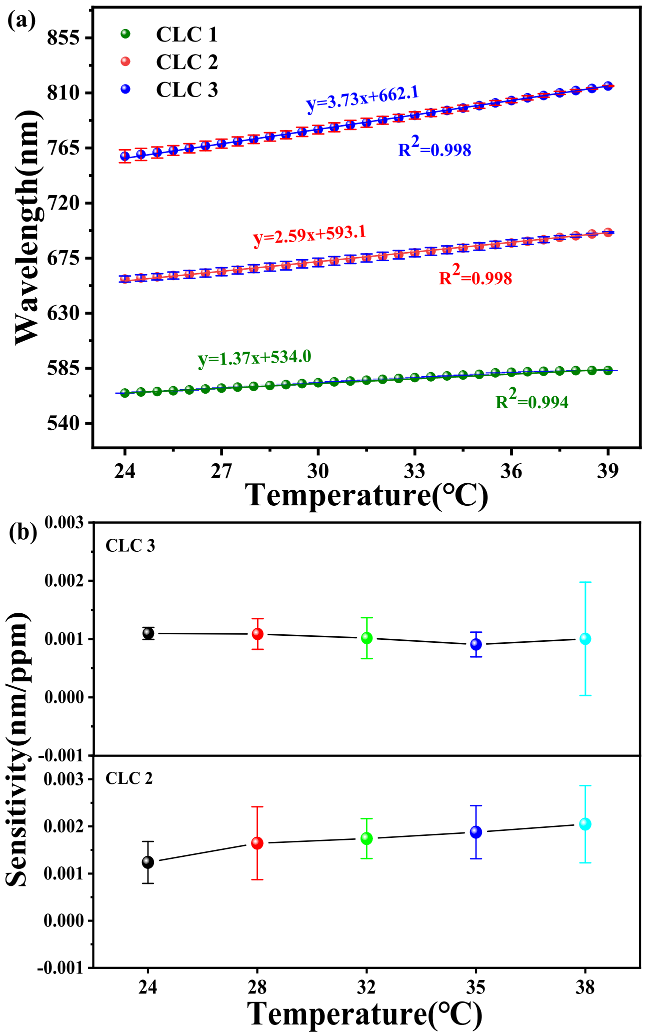

Fig. 5. (a) Linear fitting curve of different CLC with temperature. (b) Sensitivity changes of different CLCs to acetone vapor at different temperatures.

of 5 mm and a focal length of 9.99 mm. The refractive index of the cladding of the step multimode fiber is 1.4553. The refractive index of the core is 1.4733, and its numerical aperture is 0.22. The fiber has a core diameter of 105 μm and a cladding diameter of 125 μm. Fig. 4(a) is a schematic diagram of the dislocation fusion plane. The distances of the arrows indicate the fiber diameter and the distance of dislocation fusion, respectively. Fig. 4(b) is a schematic diagram of the dislocation fusion fiber. Fig. 4(c) is the energy distribution diagram of fiber dislocation fusion of 46 μm. The energy in the fiber is mainly concentrated in MMF2. While Fig. 4(e) is the energy distribution diagram of the dislocation fusion of 66 μm, and the result shows that the energy is concentrated in MMF1. Both solutions are disadvantageous when sensing measurements. Taking account of more losses of reflected light from the misaligned core, more energy was allocated to the misaligned MMF2 to guarantee similarly reflected intensities from CLC2 and CLC3. The energy distribution when the dislocation fusion is 56 μm conforms to the experimental requirements, as shown in Fig. 4(d). At the same time, the length of MMF2 is too long will increase the energy loss, and if its length

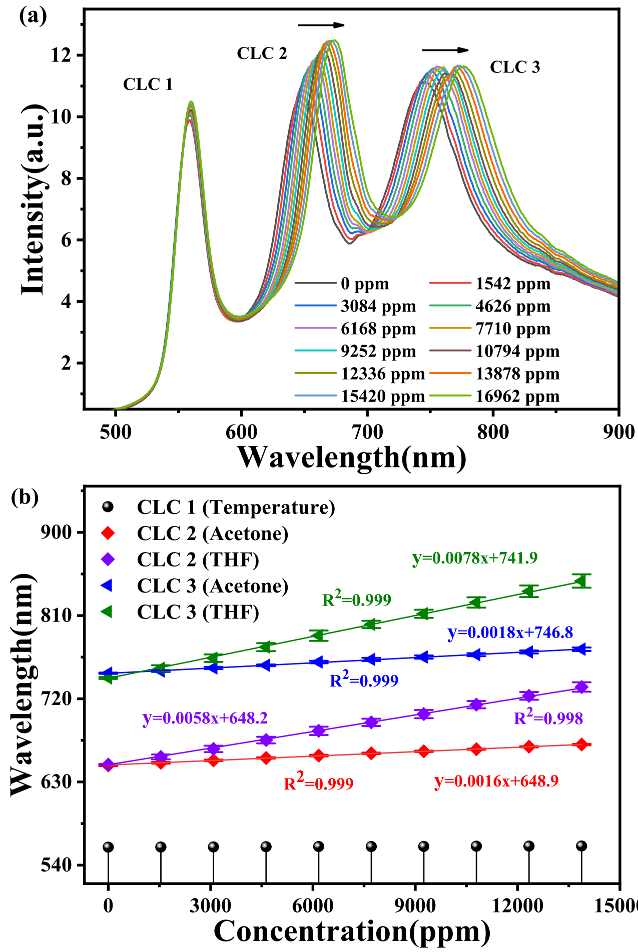

Fig. 6. (a) Reflection spectra of probes under different concentrations of acetone vapor. (b) Linear correlations between reflected wavelength and acetone as well as THF concentration.

is too short then also the two liquid crystals will be mixed. Therefore, 95 μm was finally selected.

The sensor based on CLCs can generate stable and distinct responses in temperature measurement. When measuring temperature, the sensor was placed in a small air chamber, and then control the temperature. Fig. 5(a) shows the linear correlation between different CLCs reflection spectra and temperature. After two reciprocating measurements and statistics, the experimental results showed that there is a good linear correlation between whether it is heating up or cooling down. In order to obtain accurate data, the step size was 0.2 °C/min regardless of heating or cooling. Fig. 5(b) shows the sensitivity of the sensor to acetone vapor at different temperatures. It may be because a small amount of RM257 was added to the CLCs, which caused the sensor to be less affected by temperature when exposed to organic vapor. However, the gas sensitivity of CLC2 shows a slight upward trend with temperature.

The reflection wavelength can be tuned by changing the helical pitch. When CLC is exposed to VOC, the short-range force between LC molecules is similar to the interaction force between VOC and LC. Therefore, the penetration of CLC molecules by gas molecules causes a change in the pitch (p) and ultimately changes its reflection wavelength [25]. Fig. 6(a) shows the reflection spectra corresponding to different

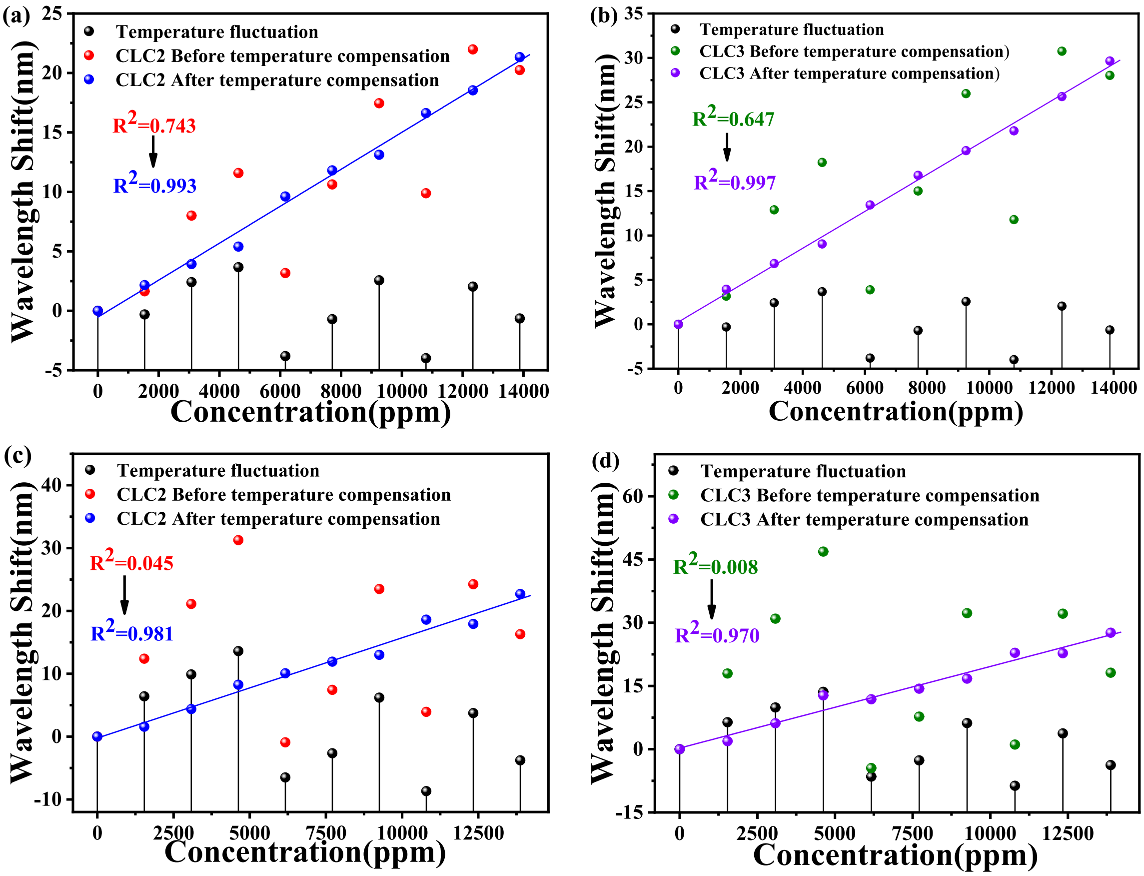

Fig. 7. The relationship between (a) CLC2 and (b) CLC3 reflected wavelength shift and acetone concentration before and after temperature compensation when the temperature fluctuates around 2 °C. The relationship between (c) CLC2 and (d) CLC3 reflected wavelength shift and acetone concentration before and after temperature compensation when the temperature fluctuates around 10 °C.

acetone concentrations monitored in real-time. The sensor was placed in the gas chamber, and acetone solution is gradually added to the gas chamber in volumes of 2 μL at a time. The reflection wavelength of the gas probe was red-shifted after acetone was completely volatilized. Since CLC1 is sealed in HCF, the slight drift of its peak only comes from temperature fluctuations. Meanwhile, the pitch of CLCs exposed to VOC gas expands. Fig. 6(b) shows the sensitivity and linear relationship of CLC2 and CLC3 to different acetone and THF concentrations. In the absence of temperature disturbance, the sensor has a good linear relationship to both acetone and THF.

To achieve the temperature compensation to CLC2 and CLC3 in gas measurement by the real-time temperature results of CLC1, firstly, the ambient temperature was changed during the measurement of organic solvent vapors. The black dots in Fig. 6 indicate the wavelength shift of the CLC1 peak due to temperature fluctuations. In order to eliminate the influence of temperature on gas detection, the solutions are given by.

$$\begin{aligned}\Delta\lambda_{CLC2_{actual}} &= \Delta\lambda_{CLC2} - \frac{\Delta\lambda_{CLC1}\cdot S_{CLC2}}{S_{CLC1}}\\ \Delta\lambda_{CLC3_{actual}} &= \Delta\lambda_{CLC3} - \frac{\Delta\lambda_{CLC1}\cdot S_{CLC3}}{S_{CLC1}}\end{aligned} \tag{1}$$

Where S_{CLC1}, S_{CLC2} and S_{CLC3} are the sensitivities of three CLCs to temperature respectively. $\Delta\lambda_{CLC1}$, $\Delta\lambda_{CLC2}$ and $\Delta\lambda_{CLC3}$ are the wavelength changes of three reflection peaks respectively, $\Delta\lambda_{CLC2\ actual}$ and $\Delta\lambda_{CLC3actual}$ are the actual wavelength for detecting different acetone concentrations after temperature compensation.

In Fig. 7(a) and Fig. 7(b), the red and green points respectively represent the wavelength shift of the CLC2 peak and CLC3 peak in response to different concentrations of acetone vapor when the temperature fluctuation range is 2 °C. Then the temperature compensation is carried out according to formula (1). The blue dots and purple dots indicate the wavelength shift of CLC2 and CLC3 after temperature compensation, respectively. The results exhibit a good linear relationship between the two CLCs reflection spectra and acetone vapor after temperature compensation, and the linear correlation coefficients are improved to 0.993 and 0.997, respectively. Fig. 7(c) and Fig. 7(d) are the response of the CLC2 peak and CLC3 peak to different concentrations of acetone vapor when the temperature fluctuant range is about 10 °C. The results showed that the optical fiber VOC gas sensor accomplishes real-time temperature monitoring as well as temperature compensation, and still keeps high accuracy and stability in an environment with temperature fluctuations. The organic solvent vapor sensitivity of CLC2 measured at different temperatures maintains an upward trend, but the sensitivity change is small, and more accurate compensation cannot be achieved.

The dynamic response time of the sensor to acetone vapor is also studied. Fig. 8(a) shows that the sensor responds faster at low acetone concentrations. The response time slightly increases at higher

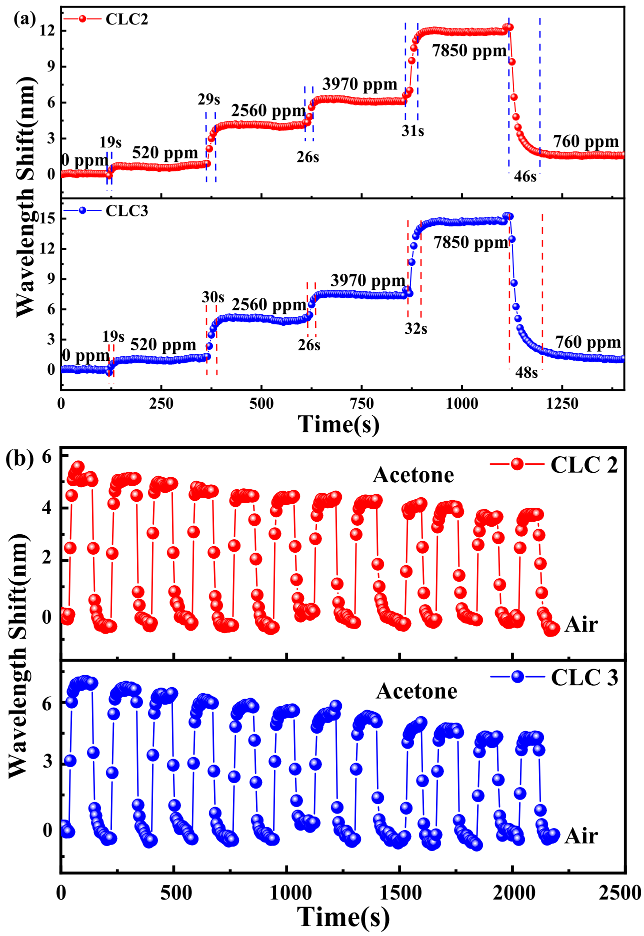

Fig. 8. (a) The dynamic response of the sensor under different concentrations of acetone vapor. (b) Dynamic response of the sensor when exposed to acetone gas.

concentrations, and its recovery time is 46 s. In short, the sensor has the characteristics of fast response and high sensitivity to VOC gas detection. Fig. 8(b) shows the repeatability of the sensor. In order to allow the acetone vapor to fully expand the CLC pitch. The probe was exposed in the gas chamber for 2 mins and then switched to air. As expected, the detection of the sensor is reversible. Here, the temperature remained almost unchanged. Every repeatable measurement will have a small amount of gas leak, which will cause a slight deviation in the measurement results. But when the optical fiber probe is exposed to air, the wavelength almost returns to its original position. Therefore, the temperature-compensated optical fiber VOC gas sensor has excellent reversibility and is a good candidate for detecting VOC in the environment.

Fig. 9(a) and Fig. 9(b) show the relationship of CLCs with different ratios of mixed gases. Since solvents with lower polarity can be more effectively combined with LCs, the interaction between them is also more obvious [25]. As far as we know, the polarity of acetone in industrial organic solvents is greater than that of THF, so the larger the proportion of THF, the more the CLC reflection peak shifts. According to the above experiment and linear correlation, the relationships between the three reflected wavelengths and temperature [26,27], total gas concentration and the gas mixing ratio can be given by.

$$\begin{bmatrix}\Delta\lambda_{CLC1}\\ \Delta\lambda_{CLC2}\\ \Delta\lambda_{CLC3}\end{bmatrix} = \begin{bmatrix}A_1 & B_1 & C_1\\ A_2 & B_2 & C_2\\ A_3 & B_3 & C_3\end{bmatrix}\begin{bmatrix}\Delta T\\ \Delta C\\ \Delta R\end{bmatrix} \tag{2}$$

Where $\Delta\lambda_{CLC1}$, $\Delta\lambda_{CLC2}$ and $\Delta\lambda_{CLC3}$ are the wavelength shifts of CLCs in response to temperature and total gas concentration, respectively; ΔT, ΔC and ΔR are temperature, total mixed gas concentration and mixed gas ratio respectively. The sensitivity coefficient of CLC1, CLC2 and CLC3 to temperature is A_i ($i = 1, 2, 3$). Similarly, B_i and C_i are the coefficients of sensitivity of three CLCs to total gas concentration and acetone/THF ratio, respectively. Therefore, the specific values of these three parameters can be obtained through the wavelength of the temperature, the total gas concentration and the ratio of the mixed gas. Fig. 9(c) and Fig. 9(d) are contour plots of $\Delta\lambda$ as a function of total gas concentration and acetone/THF ratio for the two LCs, respectively. According to the experimental results, the sensitivity coefficients were determined by linear regression, as shown in Table 2.

Stability is also an important performance of a sensor. Fig. 10 is the relationship of the two liquid crystals to acetone concentration over 11 days. In 11 days, the maximum sensitivity of CLC2 is 0.0016 nm/ppm, and the minimum sensitivity is 0.0014 nm/ppm. At the same time, the maximum sensitivity of CLC3 is 0.0021 nm/ppm, and the minimum sensitivity is 0.0018 nm/ppm. The sensitivity deviation comes from the minor difference in the acetone solvent injected into the gas chamber each time and the accumulated deviations in the selection of data points.

All in all, the performance of the VOC sensor based on dislocation fusion performs better. It responds to organic vapors such as ethanol, methanol and ethyl acetate. But the sensitivity of these organic solvents varies greatly [28] due to the different polarities of these organic solvents.

4. Conclusion

In this study, we designed a temperature-compensated optical fiber VOC gas sensor based on cholesteric liquid crystal (CLC). Real-time monitoring of temperature and mixed gas concentration is achieved by a misaligned fiber structure and three different CLCs based on the 2 × 2 multimode fiber coupler. The sensor uses the shift of the CLC reflected wavelength at different temperatures and different gas concentrations to obtain the sensitivity of temperature, acetone and tetrahydrofuran (THF). Experimental results showed that the sensor has a good linear correlation with temperature, acetone and THF. Among them, CLC1 is used to monitor changes in ambient temperature during gas detection and realize temperature compensation to eliminate the influence of temperature on gas detection results. CLC2 and CLC3 are used to detect the mixed gases of acetone and THF and realized the discrimination of two gas concentrations according to their sensitivity to different gases. In addition, the measurement results showed that the sensor has good reversibility, and can accurately detect VOC gas concentration within a relatively small temperature fluctuations extent.

CRediT authorship contribution statement

Dong Zhou: Conceptualization, Methodology, Software, Validation, Formal analysis, Writing – original draft, Writing – review & editing. **Zeqing Lan:** Validation, Formal analysis, Resources, Writing – review & editing, Supervision. **Wenzhu Cao:** Validation, Formal analysis, Supervision. **Yuzhou Chen:** Validation, Formal analysis, Supervision. **Shushen Zhang:** Supervision. **Jianyang Hu:** Validation. **Jianyu Shang:** Formal analysis. **Zenghui Peng:** Formal analysis, Supervision. **Yongjun Liu:** Validation, Formal analysis, Supervision, Project administration,

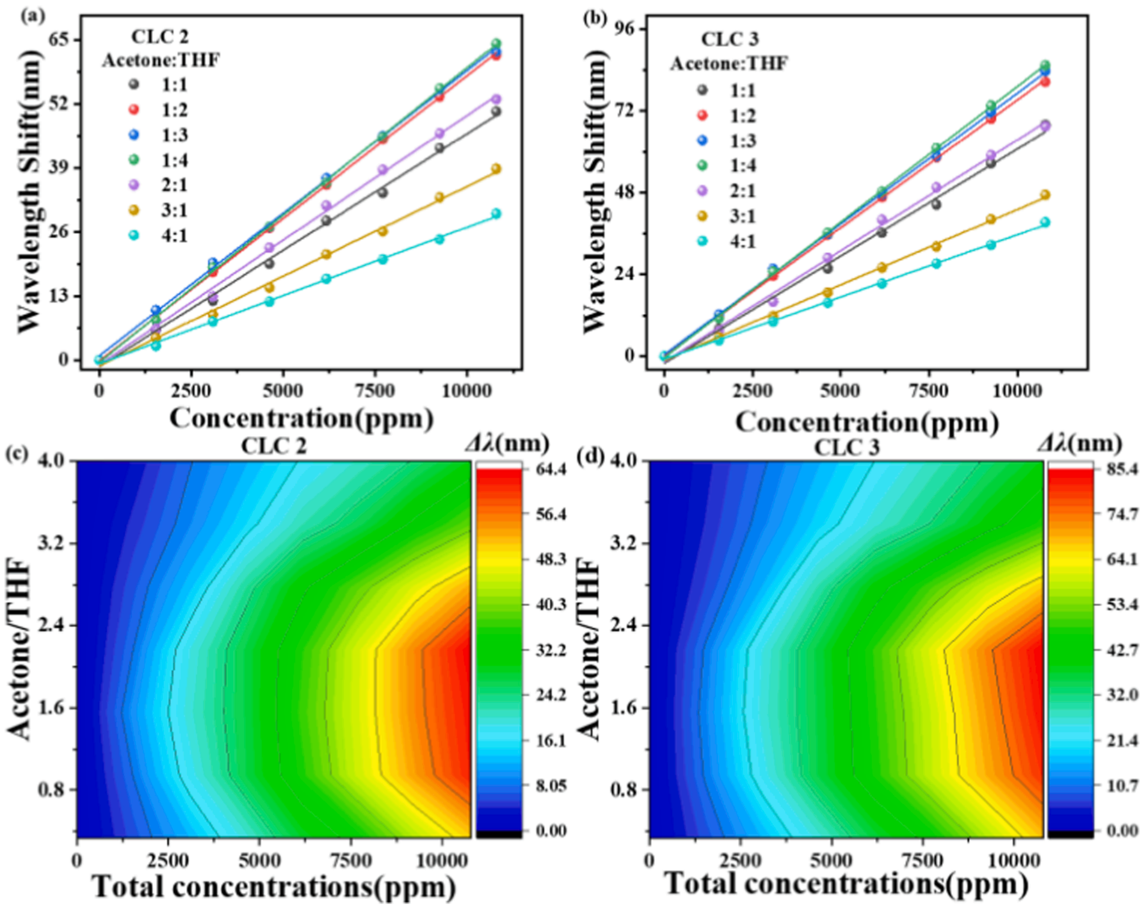

Fig. 9. The relationship between the total concentration of acetone and THF with different mixing ratios and the shift of CLC reflection wavelength. (a) The linear correlation between CLC2 and (b) CLC3 response to mixed gas. Contour plots of Δλ versus gas concentration and ratio of acetone to ethanol: (c) CLC2 and (d) CLC3.

Table 2
Sensitivity coefficient of liquid crystal to temperature, total gas concentration, acetone/THF ratio.

	CLC1	CLC2	CLC3
A_i	1.3732	2.5903	3.7312
B_i	0	0.0052	0.0068
C_i	0	−4.7517	−6.4610

Funding acquisition.

Declaration of Competing Interest

The authors declare that they have no known competing financial interests or personal relationships that could have appeared to influence the work reported in this paper.

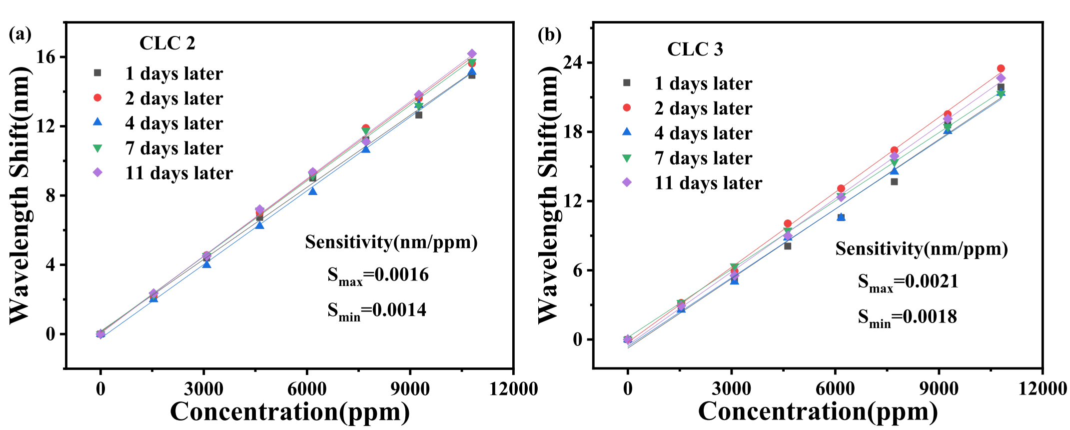

Fig. 10. Dependence of (a) CLC2 and (b) CLC3 peak wavelength shift on the acetone concentration within 11 days.

Acknowledgement

This work was financially supported by the National Science Foundation of China (Grant No. U1531102, 61775212, 61975202), the Fundamental Research Funds for the Central Universities.

References

[1] Y. Liu, P. Bai, Separation of acetone-tetrahydrofuran by extractive distillation, Chin. J. Chem. Eng. 40 (2012) 19–23.
[2] C.C. Chen, P.A. Crafts, Correlation and prediction of drug molecule solubility in mixed solvent systems with the Nonrandom Two-Liquid Segment Activity Coefficient (NRTL-SAC) model, Ind. Eng. Chem. Res. 45 (2016) 4816–4824.
[3] R. Malik, V.K. Tomer, T. Dankwort, Y.K. Mishra, L. Kienle, Cubic mesoporous Pd-WO3 loaded graphitic carbon nitride (g-CN) nanohybrids: highly sensitive and temperature dependent VOC sensors dagger, J. Mater. Chem. A 6 (2018) 10718–10730.
[4] B.F. Yu, Z.B. Hu, M. Liu, H.L. Yang, Q.X. Kong, Y.H. Liu, Review of research on air-conditioning systems and indoor air quality control for human health, Int. J. Refrig. 32 (1) (2009) 3–20.
[5] A. Mirzaei, J.-H. Kim, H.W. Kim, S.S. Kim, Resistive-based gas sensors for detection of benzene, toluene and xylene (BTX) gases: a review, J. Mater. Chem. C 6 (16) (2018) 4342–4370.
[6] H.-E. Joe, H. Yun, S.-H. Jo, M.B.G. Jun, B.-K. Min, A Review on Optical Fiber Sensors for Environmental Monitoring, Int. J. Pr. Eng. Man-GT. 5 (1) (2018) 173–191.
[7] C.L. Xia, D. Zhou, Y.M. Su, G.K. Zhou, L.S. Yao, W.M. Sun, and Y.J. Liu, A liquid-crystal-based immunosensor for the detection of cardiac troponin I, Analyst, 145 (2020) 5951-5951.
[8] A. Verdian, Z. Rouhbakhsh, E. Fooladi, An ultrasensitive platform for PCB77 detection: New strategy for liquid crystal-based aptasensor fabrication, J. Hazard. Mater. 402 (2021) 123531.
[9] W. Li, M. Khan, L. Lin, Q. Zhang, S. Feng, Z. Wu, J.-M. Lin, Monitoring H2O2 on the Surface of Single Cells with Liquid Crystal Elastomer Microspheres, Angew. Chem. Int. Edit. 59 (24) (2020) 9282–9287.
[10] Y. Zhao, Y.N. Zhang, R.Q. Lv, J. Li, Electric Field Sensor Based on Photonic Crystal Cavity With Liquid Crystal, J. Lightwave Technol. 35 (2017) 3440–3446.
[11] Y.X. Liu, C.Y. Zhao, Y.N. Zhang, G.M. Ma, X.G. Li, Y. Zhao, Electrically tunable optical fiber device based on hollow-core fiber infiltrated with liquid crystal, Sensor. Actuat. A-Phys., 318(2021) 112500.
[12] M. Humar, Liquid-crystal-droplet optical microcavities, Liq. Cryst. 43 (13-15) (2016) 1937–1950.
[13] Y. Wang, L. Zhao, A. Xu, L. Wang, L. Zhang, S. Liu, Y. Liu, H. Li, Detecting enzymatic reactions in penicillinase via liquid crystal microdroplet-based pH sensor, Sens. Actuators B Chem. 258 (2018) 1090–1098.
[14] X. Bi, D. Hartono, K.-L. Yang, Real-Time Liquid Crystal pH Sensor for Monitoring Enzymatic Activities of Penicillinase, Adv. Funct. Mater. 19 (23) (2009) 3760–3765.
[15] S.Y. Zhang, Z.J. Sun, Q.Q. Mu, Z.H. Peng, H. Liu, C. Liu, Review on liquid crystal micropolarizer array for polarization imaging, Chin. J. Liq. Crys. Disp. 37 (2022) 292.
[16] L. Sutarlie, J.Y. Lim, K.-L. Yang, Cholesteric liquid crystals doped with dodecylamine for detecting aldehyde vapors, Anal. Chem. 83 (13) (2011) 5253–5258.
[17] R.R. Shah, N.L. Abbott, Principles for Measurement of Chemical Exposure Based on Recognition-Driven Anchoring Transitions in Liquid Crystals, Science 293 (5533) (2001) 1296–1299.
[18] J. Hu, D. Zhou, Y. Su, S. Liu, P. Miao, Y. Shi, W. Sun, Y. Liu, Fiber micro-tip temperature sensor based on cholesteric liquid crystal, Opt. Lett. 45 (18) (2020) 5209.
[19] C. Zhang, D.Y. Fu, C.L. Xia, L.S. Yao, C.L. Lu, W.M. Sun, Y.J. Liu, Lasing emission of dye-doped cholesteric liquid crystal microdroplet wrapped by polyglycerol in hollow glass microsphere, Chin. Opt. Lett. 18 (2020) 011402.
[20] J. Hu, D. Fu, C. Xia, C. Zhang, L. Yao, C. Lu, W. Sun, Y. Liu, A three-layer egg-configurated Bragg microcavity of polyglycerol coated cholesteric-liquid-crystal encapsulated by hollow-glass-microsphere, Liq. Cryst. 47 (4) (2020) 508–515.
[21] P.V. Shibaev, D. Carrozzi, L. Vigilia, H. DeWeese, Liquid crystal nose, chiral case: towards increased selectivity and low detection limits, Liq. Cryst. 46 (2019) 1309–1317.
[22] L. Sutarlie, H. Qin, K.L. Yang, Polymer stabilized cholesteric liquid crystal arrays for detecting vaporous amines, Analyst 135 (2010) 1691–1696.
[23] S.S. Wang, J. Fu, M. Qiu, K.J. Huang, Z. Ma, L.M. Tong, Modeling endface output patterns of optical micro/nanofibers, Opt. Express 16 (2008) 8887–8895.
[24] Y. Zhou, Y. Huang, S.T. Wu, Enhancing cholesteric liquid crystal laser performance using a cholesteric reflector, Opt. Express 14 (2006) 3906–3916.
[25] A. Mujahid, H. Stathopulos, P.A. Lieberzeit, F.L. Dickert, Solvent Vapour Detection with Cholesteric Liquid Crystals-Optical and Mass-Sensitive Evaluation of the Sensor Mechanism, Sensors 10 (2010) 4887–4897.
[26] D. Yang, Y. Liu, Y. Wang, T. Zhang, M. Shao, D. Yu, H. Fu, Z. Jia, Integrated optic-fiber sensor based on enclosed EFPI and structural phase-shift for discriminating measurement of temperature, pressure and RI, Opt. Laser Technol. 126 (2020) 106112.
[27] S.-M. Lee, S.S. Saini, M.-Y. Jeong, Simultaneous Measurement of Refractive Index, Temperature, and Strain Using Etched-Core Fiber Bragg Grating Sensors, IEEE Photon. Technol. Lett. 22 (19) (2010) 1431–1433.
[28] K.J. Kek, J.J.Z. Lee, Y. Otono, S. Ishihara, Chemical gas sensors using chiral nematic liquid crystals and its applications, J. Soc. Inf. Display 25 (6) (2017) 366–373.